Multiple-Charge-Quanta Shot Noise in Superconducting Atomic Contacts

R. Cron, M. F. Goffman, D. Esteve, and C. Urbina

Service de Physique de l'Etat Condensé, Commissariat à l'Energie Atomique, Saclay, F-91191 Gif-sur-Yvette Cedex, France

(Received 21 December 2000)

We have measured shot noise in aluminum atomic point contacts containing a small number of conduction channels of known transmissions. In the normal state, we find that the noise power is reduced from its Poissonian value and reaches the partition limit, as calculated from the transmissions. In the superconducting state, the noise reveals the large effective charge associated with each elementary transfer process, in excellent agreement with the predictions of the quantum theory of multiple Andreev reflections.

DOI: 10.1103/PhysRevLett.86.4104 PACS numbers: 74.50.+r, 73.23.–b, 73.40.Jn, 74.40.+k

As shown already in 1924 by Shottky, the granularity of electricity gives rise to fluctuations, known as "shot noise," in the electrical current through electronic devices. Lately, a great deal of activity has been devoted to this nonequilibrium noise in coherent nanostructures connecting two charge reservoirs. It is by now evident that even its low-frequency power spectrum carries a wealth of information on the interactions and quantum correlations between the electrons [1,2] in both the charge reservoirs and the nanostructure itself. When the current I is made up from perfectly independent shots, the white noise power spectrum assumes the well-known Poissonian form $S_I = 2qI$, where q is the "effective charge" transferred at each shot. In the case of normal, i.e., nonsuperconducting, metal reservoirs, the charge of the shots is simply the electron charge e. Interactions and correlations lead to large deviations from this value. One of the most striking examples is the fractional charge of quasiparticles in the highly correlated electronic state achieved in two-dimensional electronic systems under very high magnetic fields, which was recently evidenced through noise measurements [3]. The mechanism giving rise to superconductivity is another source of correlations among electrons. How big are the shots in the current when superconducting reservoirs are involved? The current between a superconducting reservoir and a normal one connected by a short normal wire proceeds through the process of Andreev reflection in which charge is transferred in shots of $2e$, thus resulting in a doubling of the noise with respect to the normal case [4]. When two superconducting electrodes connected through structures such as tunnel junctions or short weak links are voltage biased on an energy scale eV smaller than the superconducting gap Δ, the current proceeds through multiple Andreev reflections (MAR) [5]. In a MAR process of order n, which has a threshold voltage of $V = 2\Delta/ne$, two elementary excitations are created in the electrodes while a charge ne is transferred. For a given voltage many such processes can contribute to the current, but roughly speaking, "giant" shots, with an effective charge $q \sim e(1 + 2\Delta/eV)$, are predicted at subgap energies [6]. The exact value of q, like all other transport properties of a coherent nanostructure, depends on its "mesoscopic pin code," i.e., the set of transmission coefficients $\{\tau_i\}$ characterizing its conduction channels. A full quantum theory has been developed for the fundamental case of a single conduction channel connecting two superconducting electrodes [7,8] which predicts the voltage and temperature dependence of the current noise power spectral density $s_I(V, T, \tau)$, and therefore the size of the shots, for arbitrary transmission τ. In this Letter, we present an experiment on well-characterized coherent nanostructures, namely, atomic point contacts between two superconducting electrodes, which tests quantitatively these theoretical predictions.

Using nanofabricated break junctions, we produce aluminum atomic point contacts whose sizes can be adjusted *in situ* through a mechanical control system [9]. The samples are mounted in a vacuum can and cooled below 1 K. Figure 1 shows schematically the setup used to measure both the IVs and the noise. The contact is current biased (at low frequency) through a cold resistor R_B. The bias and the voltage measurement lines are filtered by a series of microwave cryogenic distributed lossy filters, an

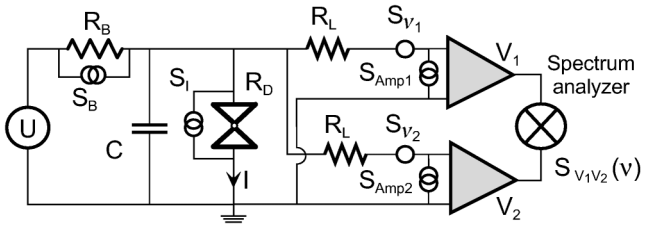

FIG. 1. Schematic experimental setup. An atomic contact (double triangle symbol), of dynamic resistance R_D, is current biased through $R_B = 1.065\ \mathrm{M}\Omega$. The voltage V across the contact is measured by two low noise preamplifiers through two nominally identical lossy lines. $R_L = (1.60 \pm 0.05)\ \mathrm{k}\Omega$ is the total resistance of each line. $C = (1.16 \pm 0.05)$ nF is the total capacitance introduced by the setup across the contact. The spectrum analyzer measures the cross-correlation spectrum of the two voltage lines. The $S_i (i = B, \mathrm{Amp1}, \mathrm{Amp2})$ are the known current noise sources associated with the bias resistor and the two amplifiers. S_I represents the signal of interest, i.e., the shot noise associated with the current through the contact. S_{v_1} and S_{v_2} represent the voltage noise sources of each line (amplifier + connecting leads).

 0031-9007/01/86(18)/4104(4)$15.00

essential requirement in order to observe MAR processes. After establishing a contact, which can be held for days, its IV characteristic is measured in the superconducting state (see inset of Fig. 4). Its code $\{\tau_i\}$ is then determined by decomposing this "mesoscopic fingerprint" [10] into the contributions of independent channels as calculated by the theory of quantum coherent MAR [11]. We work with the smallest possible contacts, which typically accommodate in aluminum three channels for a total conductance $G = G_0 \sum_i \tau_i$ of the order of the conductance quantum $G_0 = 2e^2/h$ [10]. Experiments in the normal state are done after applying a magnetic field of 50 mT, which does not affect the transmissions.

The voltage noise across the contact is measured simultaneously by two identical cascades of low noise amplifiers, and the cross spectrum $S_{V_1V_2}(\nu)$ of these two noise signals is calculated by a spectrum analyzer. This "four-point" noise measurement technique eliminates the voltage noise contributions of the resistive leads and of the preamplifiers [12]. We show in Fig. 2a examples of raw spectra $S_{V_1V_2}(\nu)$ [13] of the total noise measured at equilibrium ($I = V = 0$) and at the lowest temperature ($T = 20$ mK) for several contacts in the normal state. The spectra were measured over 800 points in a frequency window from 360 to 3560 Hz, and averaged 1000 times in typically 4 min. In this low-frequency window, the measurement lines behave as one-pole RC filters, and the cross spectrum $S_{V_1V_2}(\nu)$ adopts the form

$$S_{V_1V_2}(\nu) = \frac{R_\parallel^2}{1 + (2\pi\nu R_\parallel C)^2} \times \left[S_I + S_B + 2\left(1 + \frac{R_L}{R_\parallel}\right) S_{\mathrm{Amp}} \right]. \quad (1)$$

Here $R_\parallel = R_B R_D/(R_B + R_D)$, where $R_D(V) = \partial V/\partial I(V)$ is the dynamic resistance of the contact, which is measured simultaneously with the noise using a lock-in technique. C is the total capacitance introduced by the setup across the contact, and R_L is the total resistance of each measurement line. Besides the noise of interest, i.e., the intrinsic current noise of the contact S_I, two sources of background current noise contribute to the signal: the preamplifiers current noise $S_{\mathrm{Amp}}(\nu)$ and the white thermal current noise S_B of the bias resistor, both of which were measured independently. $S_{\mathrm{Amp}}(\nu)$ presents a linear frequency dependence almost identical for the two lines. The solid lines in Fig. 2a correspond to (1) for $V = 0$, in which case the contact contributes just its equilibrium or Johnson-Nyquist white current noise $S_I(0, T) = 4k_BT/R_D$. All measured equilibrium spectra are in agreement with what we expect from the independent characterization of our measurement setup. Therefore, in what follows we use (1) to extract from the measured $S_{V_1V_2}(\nu)$ the shot noise spectral density $S_I(V, T)$, for all contacts in both the normal and the superconducting states. We show in Fig. 2b a typical result of this analysis,

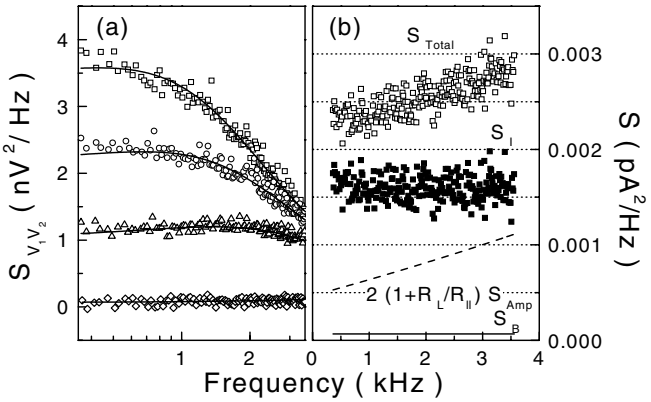

FIG. 2. (a) Measured (symbols) and calculated (solid lines) equilibrium ($V = I = 0$) cross spectra $S_{V_1V_2}(\nu)$ for four different atomic contacts in the normal state (from top to bottom: $R_D = 85.2, 64, 42, 8.5$ kΩ). The calculated spectra include the Johnson-Nyquist noise of the contacts, and the independently measured contributions of preamplifiers and bias-line current noise. They also take into account the calibrated low-pass filtering of the lines. (b) The shot noise power spectrum S_I (■) of the contact is obtained by subtracting from the total measured current noise S_{Total} (□) the two experimental sources of noise S_{Amp} and S_B. For these data, $R_D = 40.8$ kΩ and $I = 2.4$ nA.

as well as the two background contributions which are subtracted from the raw data according to (1). Within the experimental accuracy, we find that shot noise is indeed white. The average value $\langle S_I \rangle$ is the mean value of a Gaussian fit of the spectrum histogram.

The measured voltage dependence of $\langle S_I \rangle$ is shown in Fig. 3a for a typical contact in the normal state, at three different temperatures, together with the predictions of the theory of noise for quantum coherent structures [14,15],

$$S_I(V, T, \{\tau_i\}) = 2eV \coth\left(\frac{eV}{2k_BT}\right) G_0 \sum_i \tau_i(1 - \tau_i) + 4k_BTG_0 \sum_i \tau_i^2, \quad (2)$$

using the independently measured mesoscopic pin code $\{\tau_i\}$. The effective noise temperature is defined as $T^* = S_I/4k_BG$. At $V = 0$, the noise temperature is equal to T. For $eV \gg k_BT$, the noise is dominated by the nonequilibrium part, i.e., shot noise, and becomes linear in V. At $T = 0$, the predicted effective noise temperature reduces to

$$T^* = \frac{eV}{2k_B}\left(1 - \frac{\sum_i \tau_i^2}{\sum_i \tau_i}\right), \quad (3)$$

which is lower than the Poisson limit $eV/2k_B$ by the Fano factor $F(\{\tau_i\}) = 1 - \sum_i \tau_i^2/\sum_i \tau_i$. The noise measured at the lowest temperature for four contacts having different mesoscopic pin codes is shown in Fig. 3b, together with the theoretical predictions of (2). For all contacts the noise measured in the normal state is sub-Poissonian by a Fano factor, in agreement with the $\{\tau_i\}$ determined in the superconducting state. This reduction of the noise, which reflects the absence of fluctuations in the occupation

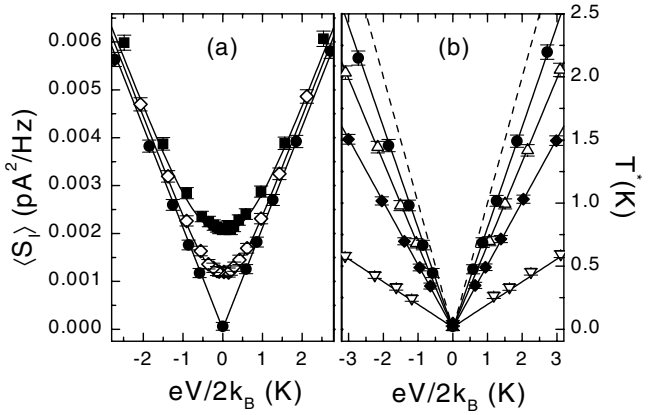

FIG. 3. (a) Symbols: measured average current noise power density $\langle S_I \rangle$ and noise temperature T^* as a function of reduced voltage, for a contact in the normal state at three different temperatures (from bottom to top: 20, 428, 765 mK). The solid lines are the predictions of (2), for the mesoscopic pin code $\{0.21, 0.20, 0.20\}$ as measured independently from the IV in the superconducting state. (b) Symbols: measured effective noise temperature T^* versus reduced voltage for four different contacts in the normal state at $T = 20$ mK. The solid lines are predictions of (2) for the corresponding mesoscopic pin codes (from top to bottom: $\{0.21, 0.20, 0.20\}$, $\{0.40, 0.27, 0.03\}$, $\{0.68, 0.25, 0.22\}$, $\{0.996, 0.26\}$). The dashed line is the Poisson limit.

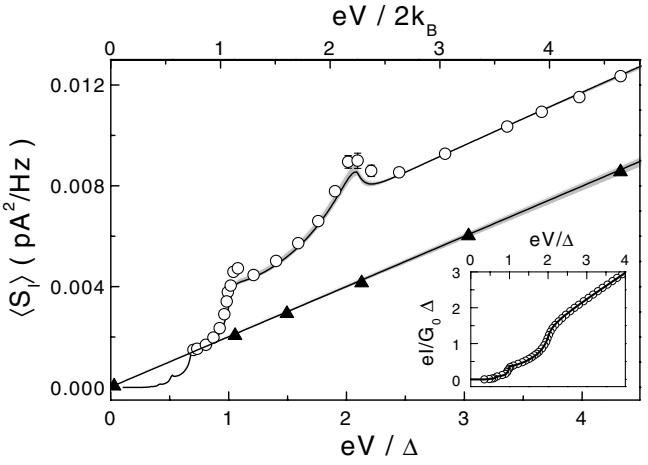

FIG. 4. Symbols: measured average current noise power density versus voltage, for a typical contact both in the normal state (triangles) and in the superconducting state (circles). Voltage is normalized to the measured superconducting gap $\Delta/e \simeq 185\ \mu$V. The solid lines are theoretical predictions, using (2) for the normal state, and using MAR noise theory for the superconducting state. The gray areas represent the fuzziness on the predicted curves due to uncertainties in the determination of the mesoscopic pin code. Inset: superconducting state IV in reduced units. The solid line is a fit to measurements (circles) using [11] and provides the mesoscopic pin code $\{0.40, 0.27, 0.03\}$ and its uncertainty used in the main panel.

numbers in the reservoirs, has already been observed in quantum point contacts tailored in 2DEG [16]. In those systems the noise originates essentially from a single channel, all the others being perfectly closed or perfectly open. On the contrary, in atomic contacts, one can have a large palette of mesoscopic pin codes, and our results constitute a first test of the general multichannel formula [17].

Having checked in the normal state the consistency between the measured shot noise reduction factor and the mesoscopic pin code determined from the IV's in the superconducting state, we then measured the noise in the superconducting state. We compare in Fig. 4, for one typical contact, the measured and the predicted $\langle S_I \rangle(V)$, in both the normal and the superconducting states. In the latter the noise is markedly nonlinear, and for high enough voltages it is above the one measured in the former. Note that these nonlinearities are not an artifact due to the voltage dependence of the dynamical resistance $R_D(V)$ entering (1), since $R_D(V)$ is measured with sufficient accuracy. The only ingredient injected into the calculated curves, $S_I(V, T, \{\tau_i\}) = \sum_i s_I(V, T, \tau_i)$, is the mesoscopic pin code $\{\tau_i\}$ extracted from the IV (see inset of Fig. 4). The agreement between experiment and the theory of MAR shot noise [7,8] is quantitative. The excess noise observed at high voltages ($V \gg 2\Delta$) in the superconducting state with respect to the normal state arises from the well-known excess current resulting from MAR processes [18].

The highly nonlinear dependence of the noise for $V < 2\Delta$ reveals the richness of the electronic transport in the superconducting state. This is visualized in Fig. 5, where the measured and the calculated effective charge $q = S_I/2I$ of the "shots" is shown as a function of inverse voltage, for four contacts spanning a large variety of mesoscopic pin codes. As can be seen, q/e does not necessarily correspond to an integer, and for a given voltage it strongly depends on the transmission of the different channels. This is due to the interfering contributions of many MAR processes of different orders. Only for very small τ's, i.e., in the tunnel regime, one expects the shots to correspond to an integer number of electrons [7,8]. Although the sensitivity of this measurement scheme does not allow us to reach this limit, the emergence of a staircase pattern shows the successive predominant role of increasing order MAR processes as the voltage decreases. Note that, for some parameters, one can have $q/e < 1$. This illustrates the fact that, as defined, the shot size not only reflects the superconducting correlations, but also the more trivial dependence of partition noise on transmissions. In other words, the Fano factor is also at play in the superconducting state. Indeed, in the limit $V \to \infty$, one expects $q/e \to F(\{\tau_i\})$. At low voltages, the effective charge diverges (see inset of Fig. 5 for contacts containing an almost ballistic channel), as has already been observed in tunnel junctions containing small defects in the insulating barrier [19] and in diffusive normal weak links [20].

We draw the following conclusions from our results. First, shot noise measurements in the normal state are in

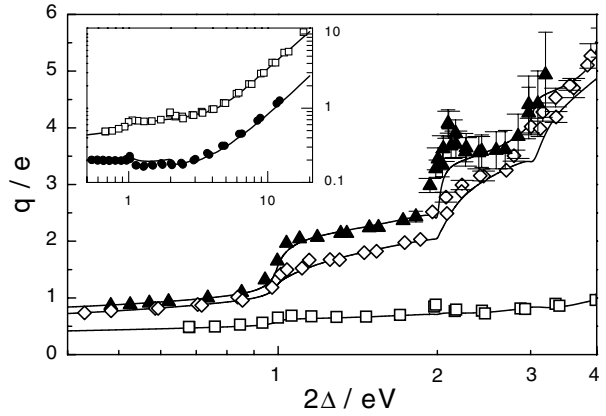

FIG. 5. Symbols: effective size $q/e = S_I/2eI$ of the noise shots versus reduced inverse voltage, for three different contacts in the superconducting state. These symbols are experimental results and the lines are predictions of the MAR theory for noise, using the mesoscopic pin codes determined from fits of the $IV's$. From top to bottom: $\{0.40, 0.27, 0.03\}$, $\{0.68, 0.25, 0.22\}$, $\{0.98, 0.55, 0.24, 0.22\}$. Inset: data for two contacts containing an almost ballistic channel (top $\{0.98, 0.55, 0.24, 0.22\}$, bottom $\{0.996, 0.26\}$) shown on a larger scale.

quantitative agreement with the independent electron multichannel theory using the $\{\tau_i\}$ determined in the superconducting state. Second, our results directly show that at finite bias voltage the microscopic current carrying processes between two superconductors do carry large effective charges. Furthermore, our results are in quantitative agreement with the predictions of the full quantum theory of MAR through a single channel. More generally, these findings, together with our previous measurements of Josephson supercurrents [21] and current-voltage characteristics [10] of superconducting atomic contacts, constitute a comprehensive positive test of the microscopic theory of superconducting transport, and firmly establish the central role of multiple Andreev reflections.

We thank M. Devoret, P. Joyez, P. F. Orfila, and H. Pothier for helpful discussions and permanent assistance. We are grateful to D. C. Glattli and P. Roche for introducing us to the subtleties of noise measurements. We also acknowledge illuminating discussions with D. Averin, J. C. Cuevas, T. M. Klapwijk, A. Levy-Yeyati, A. Martín-Rodero, Y. Naveh, V. Shumeiko, and C. Strunk. This work was partially supported by MAE through PICASSO, le Bureau National de la Métrologie, and the EU NANOMOL IST-1999-12603 project. M. F. G. acknowledges support by FOMEC.

[1] R. Landauer, Nature (London) **392**, 659 (1998).
[2] Ya. M. Blanter and M. Büttiker, Phys. Rep. **336**, 1–166 (2000).
[3] L. Saminadayar *et al.,* Phys. Rev. Lett. **79**, 2526 (1997); R. de-Picciotto *et al.,* Nature (London) **389**, 162 (1997); M. Reznikov *et al.,* Nature (London) **399**, 238 (1999).
[4] X. Jehl *et al.,* Nature (London) **405**, 50 (2000).
[5] T. M. Klapwijk, G. E. Blonder, and M. Tinkham, Physica (Amsterdam) **109B,C–110B,C**, 1657 (1982).
[6] D. Averin and H. T. Imam, Phys. Rev. Lett. **76**, 3814 (1996).
[7] J. C. Cuevas *et al.,* Phys. Rev. Lett. **82**, 4086 (1999).
[8] Y. Naveh and D. Averin, Phys. Rev. Lett. **82**, 4090 (1999).
[9] J. M. van Ruitenbeek *et al.,* Rev. Sci. Instrum. **67**, 108 (1996).
[10] E. Scheer *et al.,* Phys. Rev. Lett. **78**, 3535 (1997); E. Scheer *et al.,* Nature (London) **394**, 154 (1998).
[11] D. Averin and A. Bardas, Phys. Rev. Lett. **75**, 1831 (1995); J. C. Cuevas, A. Martín-Rodero, and A. Levy Yeyati, Phys. Rev. B **54**, 7366 (1996); E. N. Bratus' *et al.,* Phys. Rev. B **55**, 12 666 (1997).
[12] D. C. Glattli *et al.,* J. Appl. Phys. **81**, 7350 (1997).
[13] About 20 of the 800 points in the spectra corresponded to strong peaks arising from microphonics and from the power line harmonics, and are not shown for clarity.
[14] G. B. Lesovik, Sov. Phys. JETP Lett. **49**, 592 (1989).
[15] Th. Martin and R. Landauer, Phys. Rev B **45**, 1742 (1992); M. Büttiker, Phys. Rev. B **46**, 12 485 (1992).
[16] M. Reznikov *et al.,* Phys. Rev. Lett. **75**, 3340 (1995); A. Kumar *et al.,* Phys. Rev. Lett. **76**, 2778 (1996).
[17] This reduction below Poissonian noise has already been used to obtain partial information on the mesoscopic pin code of normal atomic contacts [H. E. van den Brom and J. M. van Ruitenbeek, Phys. Rev. Lett. **82**, 1526 (1999)].
[18] J. P. Hessling *et al.,* Europhys. Lett. **34**, 49 (1996).
[19] P. Dieleman *et al.,* Phys. Rev. Lett. **79**, 3486 (1997).
[20] T. Hoss *et al.,* Phys. Rev. B **62**, 4079 (2000).
[21] M. F. Goffman *et al.,* Phys. Rev. Lett. **85**, 170 (2000).